Binding of Δ- and Λ-$[Ru(phen)_3]^{2+}$ to $[d(CGCGATCGCG)]_2$ Studied by NMR†

Magdalena Eriksson,*,‡ Mikael Leijon,§ Catharina Hiort,∥ Bengt Nordén,∥ and Astrid Gräslund§

Department of Medical Biophysics and Biochemistry, University of Umeå, S-901 87 Umeå, Sweden, Department of Biophysics, Arrhenius Laboratory, University of Stockholm, S-106 91 Stockholm, Sweden, and Department of Physical Chemistry, Chalmers University of Technology, S-412 96 Göteborg, Sweden

Received October 27, 1993; Revised Manuscript Received February 9, 1994®

ABSTRACT: The interactions of the Δ and Λ enantiomers of the chiral metal complex $[Ru(phen)_3]^{2+}$ (phen = 1,10-phenanthroline) with the oligonucleotide duplex $[d(CGCGATCGCG)]_2$ have been studied with NMR and CD spectroscopy. From NOESY data it is shown that the interaction primarily takes place in the minor groove of the oligonucleotide which remains in a B-like conformation. The observed NOEs also provide evidence that the metal complexes preferentially bind to the central AT region. The observed AT specificity is more pronounced with the Δ as compared to the Λ enantiomer, which interacts with a larger part of the oligonucleotide. Furthermore, the NOESY data show that neither of the enantiomers binds by classical intercalation. This is also supported by a comparison study of the analogue $[Ru(phen)_2DPPZ]^{2+}$ (DPPZ = dipyrido[3,2-*a*:2′,3′-*c*]phenazine) which intercalates in DNA. The NMR as well as the CD results show that the Δ and Λ enantiomers of $[Ru(phen)_3]^{2+}$ bind in different modes to $[d(CGCGATCGCG)]_2$. Comparison of CD spectra of the metal complex in the presence of $[d(CGCGATCGCG)]_2$, poly(dAdT)·poly(dAdT), poly(dGdC)·poly(dGdC), and calf thymus DNA suggests that these binding modes are independent of DNA sequence. The results are found to be compatible with binding of Δ-$[Ru(phen)_3]^{2+}$ by insertion of two phenanthroline ligands into the minor groove, causing minor distortions of the DNA structure, whereas the Λ enantiomer binds in a mode that leaves the DNA structure unaffected.

The chiral transition metal complex $[Ru(phen)_3]^{2+}$ (phen = 1,10-phenanthroline)[1] appears in two inversion-stable forms, the Δ and Λ enantiomers (I and II, respectively). These can

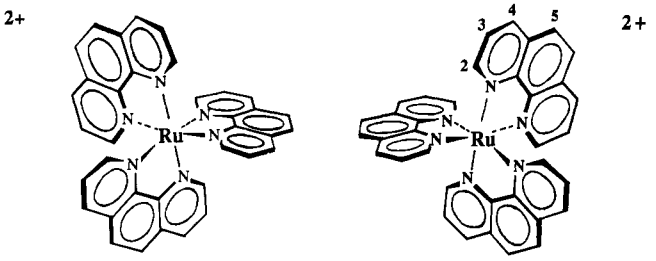

I II

be described as right- and left-handed propellers, respectively, with the phenanthroline ligands constituting the propeller blades, octahedrally coordinated by the metal ion. Δ- and Λ-$[Ru(phen)_3]^{2+}$ both bind to DNA, but their affinities as well as the enantioselectivity depend on the DNA sequence (Barton et al., 1986; Hiort et al., 1990).

Metal complexes like $[Ru(phen)_3]^{2+}$ and their interactions with DNA have attracted increasing interest for a number of reasons. First, it has been suggested that the chiral complexes can be used as structural probes, discriminating between right- and left-handed DNA (Barton et al., 1983; Barton, 1984). However, chiral discrimination with $[Ru(phen)_3]^{2+}$ has been questioned, since the metal complex induces a local transition from Z- to B-conformation upon binding to poly(dGm^{5}dC)·poly(dGm^{5}dC) (Härd et al., 1987). Second, several transition metal complexes of this type have the ability to mediate light-induced DNA single-strand cleavage and thus may have potency as chemical endonucleases (Barton & Raphael, 1984; Sitlani et al., 1992). Third, it has been suggested that $[Ru(phen)_3]^{2+}$ binds to the major groove of DNA (Barton et al., 1986; Hiort et al., 1990; Haworth et al., 1991). Major groove binding of drug molecules is rarely reported, and its nature is still poorly understood. Furthermore, the binding of $[Ru(phen)_3]^{2+}$ to DNA is relatively weak (Hiort et al., 1990; Satayanarayana et al., 1992; Barton et al., 1984b), and the exchange rate between the bound and free states is rapid on the NMR time scale at temperatures above 20 °C (Eriksson et al., 1992; Rehmann & Barton, 1990a), yielding sharp peaks for all nonexchangeable protons in the NMR spectrum. This is in contrast to most intercalators which have binding kinetics in the intermediate exchange range and give rise to broad peaks for the protons affected by the drug.

Extensive efforts have been made to gain insight into the structural properties of the binding of $[Ru(phen)_3]^{2+}$ to DNA. For both enantiomers, the major questions have been where the binding takes place, externally at the phosphate–sugar backbone or at the surface in either of the grooves; whether one of the phenanthroline ligands intercalates or not; and what sequence specificity there is. Barton and co-workers have, on the basis of luminescence and NMR studies, proposed two binding modes, one surface bound in the minor groove and one intercalated from the major groove (Rehmann & Barton, 1990b). Both enantiomers were suggested to bind predominantly in the surface mode. Hiort et al. have argued, from linear and circular dichroism studies, in favor of major groove binding for both enantiomers (Hiort et al., 1990). Major

† This study was supported by the Swedish Natural Science Research Council and the Magn. Bergwall Foundation.

‡ University of Umeå.

§ University of Stockholm.

∥ Chalmers University of Technology.

® Abstract published in *Advance ACS Abstracts,* April 1, 1994.

[1] Abbreviations: $[Ru(phen)_3]^{2+}$, tris(1,10-phenanthroline)ruthenium(2+); $[Ru(phen)_2DPPZ]^{2+}$, bis(1,10-phenanthroline)(dipyrido[3,2-*a*:2′,3′-*c*]phenazine)ruthenium(2+); *r*, metal complex/oligonucleotide duplex concentration ratio.

0006-2960/94/0433-5031$04.50/0

groove binding for both enantiomers has also been supported by molecular modeling and energy minimization including solvent effects (Haworth et al., 1991). Recently, however, evidence for minor groove binding of $[Ru(phen)_3]^{2+}$ was found. From two-dimensional NMR results it was shown that both the Δ and Λ enantiomers of $[Ru(phen)_3]^{2+}$ bind in the minor groove of the oligonucleotide $[d(CGCGATCGCG)]_2$ (Eriksson et al., 1992). Strong indications for nonintercalative binding were also found. Here we present an extended NMR study of the $[Ru(phen)_3]^{2+}$–oligonucleotide interaction. We present new evidence for nonintercalative binding in the minor groove, and a comparison is made with the DNA-binding properties of the analogue $[Ru(phen)_2DPPZ]^{2+}$ (DPPZ = dipyrido[3,2-*a*:2′,3′-*c*]phenazine, III), which has been shown

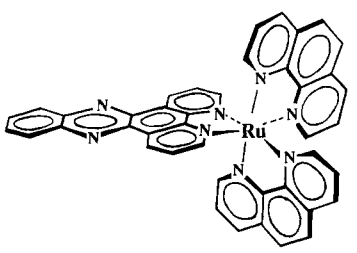

III

to intercalate (Friedman et al., 1990; Hiort et al., 1993). The binding constants for Δ- and Λ-$[Ru(phen)_3]^{2+}$ to $[d(CGCGATCGCG)]_2$ have been estimated, and the differences between the two $[Ru(phen)_3]^{2+}$ enantiomers, regarding DNA sequence specificity and binding modes, are discussed. In addition, we present CD results on $[Ru(phen)_3]^{2+}$ interacting with oligonucleotides, calf thymus DNA, and synthetic polynucleotides, and the results are discussed in terms of general DNA-binding modes of these metal complexes.

MATERIALS AND METHODS

$RuCl_3$ was obtained from Aldrich Chemical Co. Inc. Racemic $[Ru(phen)_3]^{2+}$ was synthesized and separated into chiral isomers according to Dwyer and Gyarfas (1949). The concentration of $[Ru(phen)_3]^{2+}$ was spectroscopically determined using a molar extinction coefficient of 19 000 M^{-1} cm^{-1} at 447 nm. Chemical and enantiomeric purity was certified by CD and light absorption measurements. The Δ and Λ enantiomers were of 95% and 99% enantiomeric purity, respectively. Enantiomerically pure DPPZ was synthesized as described by Hiort et al. (1993). The oligonucleotide d(CGCGATCGCG) was purchased from Symbicom AB (Umeå, Sweden). For the NMR experiments oligonucleotide concentrations of 1.1–1.4 mM (duplex) and a 10 mM phosphate buffer solution, pH = 7.0, were used. For the CD experiments the nucleotide concentration was 0.30 mM (phosphate), and a 1 mM cacodylate buffer, pH = 7.0, containing 10 mM NaCl was used.

NMR experiments were performed on a Bruker AM 500 spectrometer. For samples in D_2O presaturation was used to suppress the H_2O residual peak, and for samples in H_2O a 1:3:3:1 pulse sequence was used for water suppression. Phase-sensitive NOESY data were acquired with time-proportional phase incrementation, using various mixing times. Fourier transformation and further processing of NMR data were done with the Felix software package (version 2.1, Hare Research Inc.). CD spectra were recorded on a Jasco J-720 spectropolarimeter.

Determination of Binding Constants. The equilibrium constant for the reaction L + DNA = L–DNA can be written as

$$K = \frac{[L - DNA]}{[L][DNA]} \quad (1)$$

where L and DNA symbolize ligand and DNA binding site, repectively. The concentration ratio of ligand and DNA binding sites, r, is given by

$$r = \frac{[L] + [L - DNA]}{[DNA] + [L - DNA]} \quad (2)$$

The chemical shift, δ, of a DNA proton in a magnetic environment that changes rapidly due to ligand binding (chemical exchange that is rapid on the NMR time scale) can be expressed as

$$\delta = x_f\delta_f + x_b\delta_b \quad (3)$$

where x_f and x_b are the fractions of the DNA proton in the free and bound states, respectively, and δ_f and δ_b are the corresponding chemical shifts. With the total concentration of DNA binding sites, c = [DNA] + [L–DNA], eq 2 can be rewritten as

$$r = \frac{Kc + (\delta_b - \delta_f)/(\delta_b - \delta)}{Kc[(\delta_b - \delta_f)/(\delta - \delta_f)]} \quad (4)$$

This equation describes r as a function of δ, with K and δ_b as parameters to be fitted. Nonlinear regression then gives estimates of K and δ_b. Equation 4 can be rewritten as

$$x_b = \frac{r + 1 + (Kc)^{-1}}{2} - \left\{\frac{[r + 1 + (Kc)^{-1}]^2}{4} - r\right\}^{1/2} \quad (5)$$

and the fitting of the binding parameters can graphically be represented by plotting x_b $[=(\delta - \delta_f)/(\delta_b - \delta_f)]$ vs r.

RESULTS

One-Dimensional NMR Experiments. The interactions of the Δ and Λ enantiomeric forms of $[Ru(phen)_3]^{2+}$ with $[d(CGCGATCGCG)]_2$ have been studied with ^1H NMR. Figure 1 shows the aromatic region of the spectrum of the oligonucleotide as titrated with Δ-$[Ru(phen)_3]^{2+}$. An important observation is that there is only one set of resonances in the spectrum. This shows that the metal complex exchanges rapidly on the NMR time scale; i.e., the free and bound states are indistinguishable. Furthermore, it shows that the three phenanthroline moieties are equivalent and protons **2**, **3**, **4**, and **5** are equivalent to protons **9**, **8**, **7**, and **6**, respectively.

The resonances of the phenanthroline protons of both Δ- and Λ-$[Ru(phen)_3]^{2+}$ as well as most of the DNA protons were assigned. The phenanthroline protons were assigned by identification of their splitting patterns; proton **3** appears as a triplet and **5** as a singlet, while protons **2** and **4** are doublets. These doublet peaks were distinguished by inference of NOESY and COSY experiments (COSY data not shown).

All phenanthroline protons shift upfield upon binding to the oligonucleotide. The shift amplitude is much larger for the Δ enantiomer, with the largest effect for proton **5**, for which a shift difference of nearly 0.3 ppm between the free and bound states is observed. When the NaCl concentration was raised from 10 to 50 mM, downfield shifts of the phenenthroline protons (0.07 ppm for **5**) were observed (data

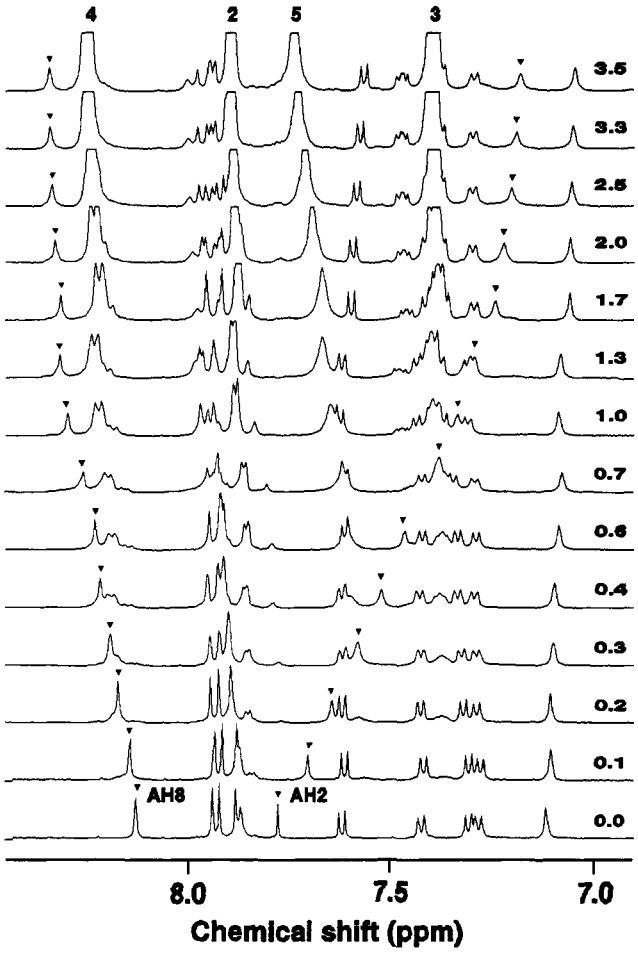

FIGURE 1: Aromatic region of the ^1H NMR spectrum of Δ-$[Ru(phen)_3]^{2+}$ and $[d(CGCGATCGCG)]_2$ in D_2O solution at 41 °C. The resonances of the phenanthroline protons, H2 and H8 of A2, and the *r*-values are indicated.

not shown), in response to the reduced electrostatic attraction experienced by the metal complex, as has previously been discussed (Barton et al., 1986; Hiort et al., 1990; Satayanarayana et al., 1992).

Large chemical shift changes are seen for some of the oligonucleotide protons when they interact with the Ru complexes. For example, the aromatic proton H2 of A5 is strongly affected and shifts extensively upfield upon addition of either enantiomer of $[Ru(phen)_3]^{2+}$, as seen for Δ in Figure 1. This shows that H2(A5) experiences a changing magnetic environment upon binding to the metal complex, most likely due to ring current effects from closely located phenanthrolines, possibly in combination with smaller changes in the base-pair stacking, such as inter-base-pair shifting, sliding, or changes in the helical twist. Many of the sugar protons are also affected by ligand binding. Figure 2 shows the chemical shift changes of the sugar H1′ and aromatic H6/H8 protons upon addition of Δ- and Λ-$[Ru(phen)_3]^{2+}$ to concentration ratios, *r*, of 2.7 and 3.5, respectively. The H1′ protons around the central region of the oligonucleotide are strongly affected and exhibit considerable upfield shifts. It should be noticed that the effect of the Δ enantiomer is essentially limited to residue T6 while the effect of the Λ enantiomer extends over G4 and A5 as well. Smaller shift changes are observed for the major groove aromatic protons H6 and H8, but no clear trend can be seen. The H5 protons of residues C7 and C3 exhibit large downfield shift changes (about 0.3 ppm) with the Δ enantiomer that are likely due to minor changes in the base-pair stacking. Smaller downfield shifts are observed for the methyl protons of T6 as

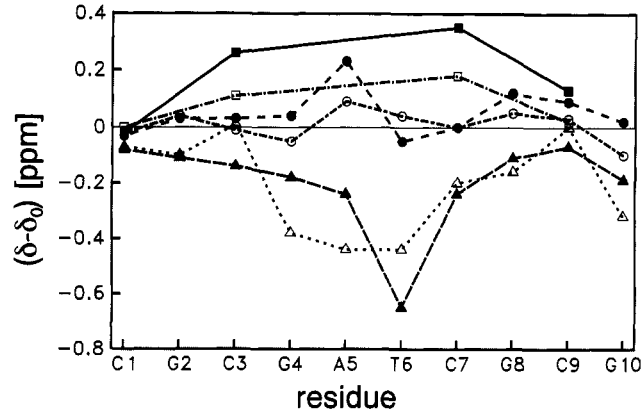

FIGURE 2: Chemical shift changes of protons of [d(CGCGATCGCG)]$_2$ interacting with Δ-$[Ru(phen)_3]^{2+}$ (r = 2.7) (filled symbols) and Λ-$[Ru(phen)_3]^{2+}$ (r = 3.5) (open symbols), at 41 °C: H5 protons (□), H6 or H8 protons (○), and H1′ protons (△).

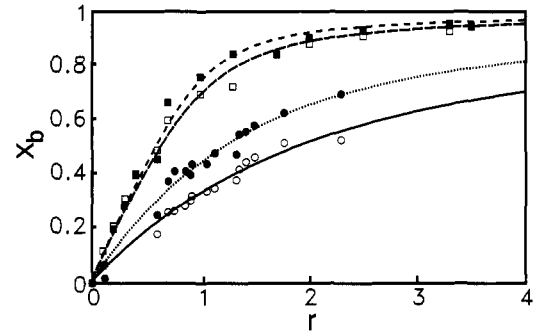

FIGURE 3: Fraction of oligonucleotide protons H2(A5) (open symbols) and H8(A5) (filled symbols) interacting with $[Ru(phen)_3]^{2+}$, x_b, as a function of the *r*-value, according to eq 5. Titration with Δ-$[Ru(phen)_3]^{2+}$ (□) and with Λ-$[Ru(phen)_3]^{2+}$ (○).

$[Ru(phen)_3]^{2+}$ is added, an effect that is stronger with the Δ than with Λ enantiomer (results not shown). It is clear that, with the Δ enantiomer, the most pronounced changes in chemical shifts of the oligonucleotide protons take place around the A5·T6 base pairs. With the Λ enantiomer similar, but less pronounced, effects are seen also in the flanking G4·C7 base pair. These observations can be taken as evidence for preferential binding of both Δ- and Λ-$[Ru(phen)_3]^{2+}$ to the central AT region of $[d(CGCGATCGCG)]_2$, in agreement with prevoius reports (Eriksson et al., 1992).

Binding Constants. The binding constants of Δ- and Λ-$[Ru(phen)_3]^{2+}$ to the AT region of $[d(CGCGATCGCG)]_2$ were determined from the chemical shift changes observed for H2(A5) and H8(A5) upon titration with the metal complexes. As described in Materials and Methods, the binding data were fitted to eq 4, which gives estimates of the parameters K and δ_b. Using these results conventional binding curves were plotted according to eq 5 (Figure 3). The binding constants evaluated were $K_{H2(A5)} = 7.5 \times 10^3\ M^{-1}$ and $K_{H8(A5)} = 11.5 \times 10^3\ M^{-1}$ for the Δ enantiomer and $K_{H2(A5)} = 0.6 \times 10^3\ M^{-1}$ and $K_{H8(A5)} = 1.2 \times 10^3\ M^{-1}$ for the Λ enantiomer. Averaging these values gives $K_{\Delta\text{-AT}} = 1.0 \times 10^4\ M^{-1}$ and $K_{\Lambda\text{-AT}} = 1.0 \times 10^3\ M^{-1}$. It should be noted that the binding constants determined here exclusively measure metal complex binding that affects the observed protons H2 and H8 of A5 and is oblivious to any other type of binding. The values of K are thus determined with the assumption that ligand binding exclusively occurs to the minor groove AT site. Binding to any other site would lower the concentration of the free ligand and thus increase the value of K. Therefore, the values obtained represent lower limits of the binding constants.

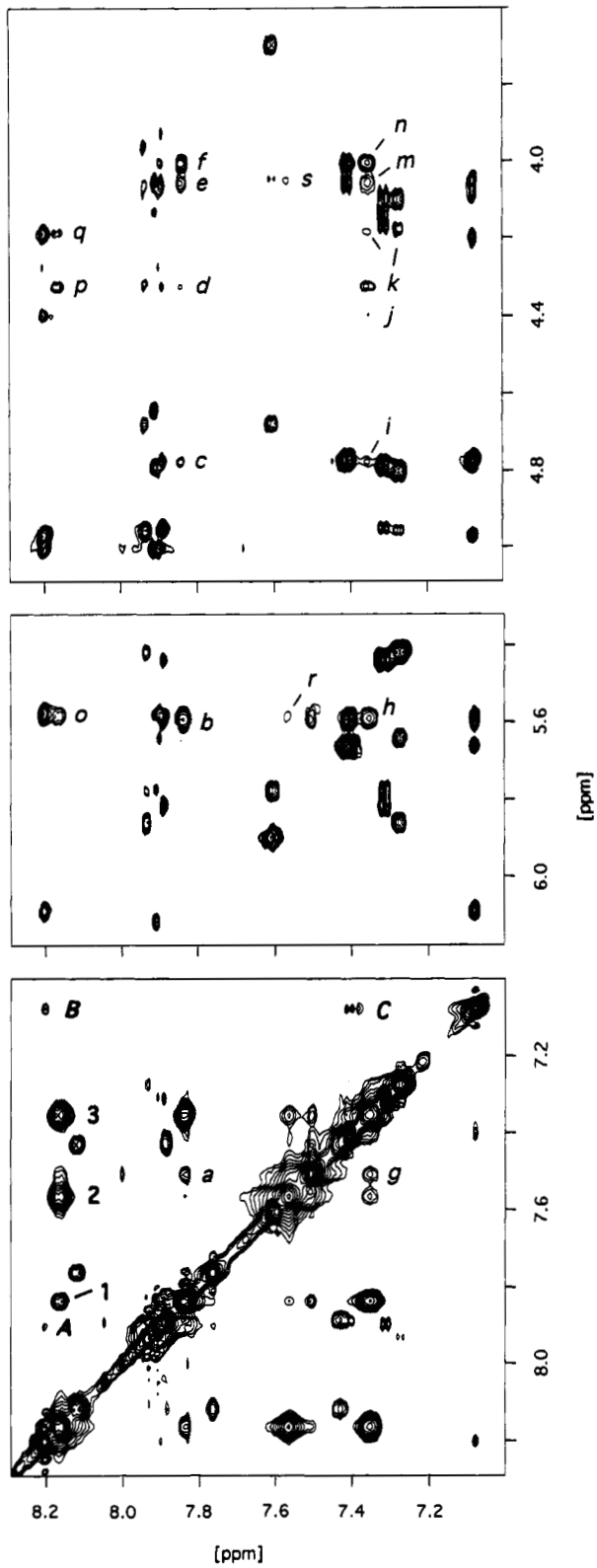

FIGURE 4: NOESY spectrum of Δ-$[Ru(phen)_3]^{2+}$ and [d(CGCGATCGCG)]$_2$ at concentration ratio = 0.5 (1.1 mM duplex concentration) in D_2O solution at 41 °C, with mixing time = 450 ms. Panels: aromatic–aromatic region (lower), aromatic–H1′ region (center), and aromatic–H3′,H4′,H5′,H5″ region (upper). Labeling of cross-peaks: **4–2**, 1; **4–5**, 2; **4–3**, 3; H8(G4)–H8(A5), A; H8(A5)–H6(T6), B; and H6(T6)–H6(C7), C; the rest as in Table 1.

Two-Dimensional NMR Experiments. Two-dimensional NOESY experiments were carried out at various [Ru(phen)$_3$]$^{2+}$/oligonucleotide concentration ratios. In Figure 4 parts of a NOESY spectrum of Δ-[Ru(phen)$_3$]$^{2+}$ and [(CGCGATCGCG)]$_2$ at a concentration ratio of r = 0.5 are shown. The corresponding spectrum with the Λ enantiomer at r = 2.3 is shown in Figure 5. These spectra were selected because at these r-values the spectral overlap of phenanthroline and DNA protons is relatively small and the intermolecular cross-peaks can easily be seen. Furthermore, the degree of occupancy of the AT site is comparable for the two enantiomers (approximately 0.5), as judged by the relative shift changes; see Figure 3. Experiments were performed at various mixing times, but in order to study intermolecular interactions, data were mostly collected at long mixing times, such as 450 ms. This is because of the slow buildup rates of intermolecular cross-peaks; the rapid exchange of the ligands makes the effective mixing time for phenanthroline–DNA proton interactions significantly shorter than the nominal mixing time.

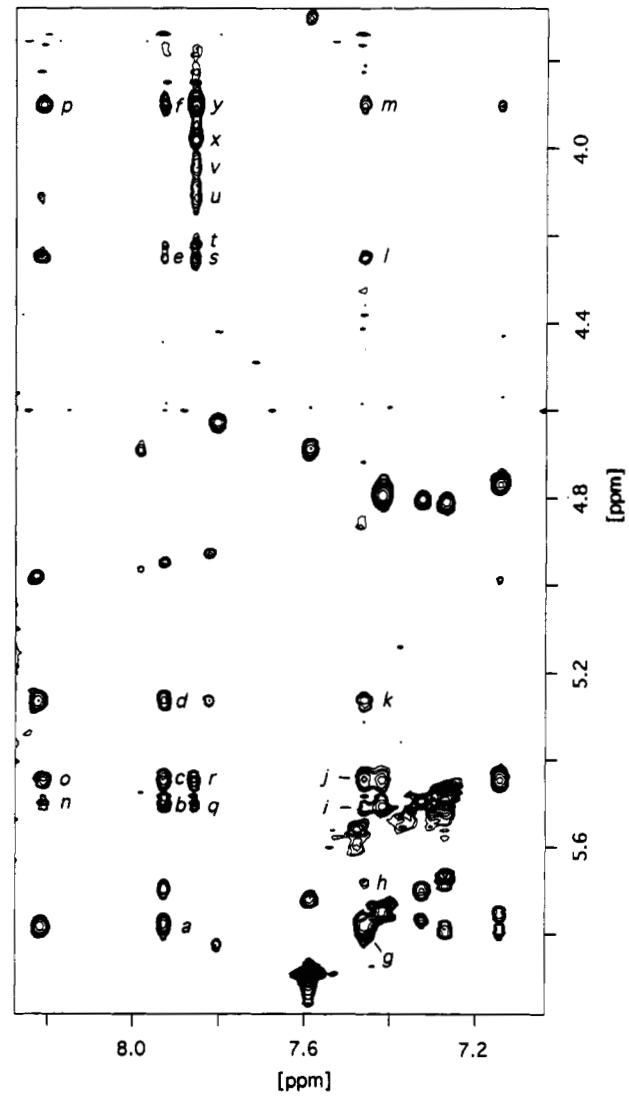

FIGURE 5: NOESY spectrum of Λ-$[Ru(phen)_3]^{2+}$ and [d(CGCGATCGCG)]$_2$ at concentration ratio = 2.3 (1.4 mM duplex concentration) in D_2O solution at 41 °C, with mixing time = 200 ms. The aromatic–H1′,H3′,H4′,H5′,H5″ region is shown. Labeling of cross-peaks is as in Table 2.

With both Δ- and Λ-$[Ru(phen)_3]^{2+}$ the oligonucleotide exhibits regular B-form cross-peak patterns in the NOESY spectra. This indicates that no major distortions of the oligonucleotide structure result from the metal complex interaction. In the aromatic–aromatic region strong NOE cross-peaks are seen among the phenanthroline protons, as seen in Figure 4 for the Δ form. The relative intensities of the intra-phenanthroline cross-peaks were useful for the assignment of these protons. The spectrum with the Δ

Table 1: NOE Cross-Peaks Observed between Δ-$[Ru(phen)_3]^{2+}$ and $[d(CGCGATCGCG)]_2$ at $r = 0.5$ in D_2O Solution Containing 10 mM Phosphate Buffer, pH = 7.0, and 10 mM NaCl, 41 °C

2–H2(A5)	medium	a
2–H1′(G4/T6/C7)	strong	b
2–H3′(T6/C7)	weak	c
2–H4′(G2/G8)	weak	d
2–H4′/H5′/H5″(T6/C7)	medium	e
2–H4′(C7)	strong	f
3–H2(A5)	weak	g
3–H1′(G4/T6/C7)	medium	h
3–H3′(T6/C7)	weak	i
3–H4′(A5)	weak	j
3–H4′(G2/G8)	weak	k
3–H4′/H5′/H5″(A5/T6)	weak	l
3–H4′/H5′/H5″(A5/T6/C7)	weak	m
3–H4′(C7)	medium	n
4–H1′(G4/T6/C7)	medium	o
4–H4′(G2/G8)	medium	p
4–H4′/H5′/H5″(A5/T6)	weak	q
5–H1′(G4/T6/C7)	weak	r
5–H4′/H5′/H5″(T6/C7/G8)	weak	s

Table 2: NOE Cross-Peaks Observed between Δ-$[Ru(phen)_3]^{2+}$ and $[d(CGCGATCGCG)]_2$ at $r = 2.3$ in D_2O Solution Containing 10 mM Phosphate Buffer, pH = 7.0, and 10 mM NaCl, 41 °C

2–H2(A5)	medium	
2–H1′(A5)	strong	a
2–H1′(C7)	medium	b
2–H1′(T6)	medium	c
2–H1′(G4)	medium	d
2–H4′(A5)	weak	e
2–H4′(T6)	medium	f
3–H2(A5)	weak	
3–H1′(A5)	strong	g
3–H1′(C3)	weak	h
3–H1′(C7)	weak	i
3–H1′(T6)	medium	j
3–H1′(G4)	medium	k
3–H4′(A5)	medium	l
3–H4′(T6)	medium	m
3–H2′(A5)	weak	
3–H2″(A5)	weak	
4–H1′(C7)	medium	n
4–H1′(T6)	medium	o
4–H4′(T6)	strong	p
4–H2″(C7)	weak	
5–H1′(C7)	medium	q
5–H1′(T6)	medium	r
5–H4′(A5)	medium	s
5–H4′(G8)	medium	t
5–H4′(G4)	medium	u
5–H4′(C3)	medium	v
5–H4′(C7)	strong	x
5–H4′(T6)	strong	y

enantiomer (Figure 4) exhibits a second, weaker, set of cross-peaks which is due to remnants of the Λ enantiomer present in the sample. Sequential cross-peaks between the DNA base protons are also observed, represented by peaks A, B, and C in Figure 4. This indicates that the base-pair stacking is maintained in the oligonucleotide when it interacts with the metal complex.

For both Δ- and Λ-$[Ru(phen)_3]^{2+}$ we see several NOE interactions with the oligonucleotide protons which are listed in Tables 1 and 2, respectively. With Δ-$[Ru(phen)_3]^{2+}$ we observe cross-peaks between the phenanthroline protons **2** and **3** and the aromatic proton H2 of A5 (labeled a and g, respectively, in Figure 4). We also see NOEs between **2**, **3**, **4**, and **5** and the sugar protons H1′, H3′, and H4′ of G4, A5, T6, and C7. Because of spectral overlaps, the H4′, H5′, and H5″ protons within some of the residues cannot be unambiguously assigned. In addition, weak interactions are seen to H4′ sugar protons on the G2 and/or G8 residues.

A similar cross-peak pattern is observed with the Λ enantiomer (Figure 5). Protons **2** and **3** show NOE cross-peaks to H2 of A5, and all four ligand protons exhibit interactions with the H1′, H3′, and H4′ sugar protons of G4, A5, T6, and C7. At higher r-values weak cross-peaks to the G2, C3, and G8 residues are seen. A few weak NOEs to H2′ and H2″ protons are observed at $r > 2.0$. These are most likely due to spin diffusion from adjacent H1′ protons which show much stronger interactions with the phenanthroline.

A number of interesting observations may be noticed at this point. First, with Δ-$[Ru(phen)_3]^{2+}$ fewer and weaker cross-peaks between protons **4** and **5** and the oligonucleotide are seen, as compared to the Λ-enantiomer. Second, the cross-peaks to the H1′ and H4′ protons are, with both Δ and Λ, much more intense than the ones to the H3′, H2′, and H2″ protons. Third, the Δ enantiomer shows fewer NOE interactions to the sugar protons on A5 compared to the surrounding residues G4, T6, and C7, which is not the case with the Λ enantiomer.

The aromatic proton H2 of adenine and the sugar protons H1′ and H4′ are located in or around the minor groove in B-form DNA. It should be noticed that no NOE contacts are observed to any of the protons located in the major groove, i.e., the aromatic protons H5, H6, and H8 and the thymine methyl protons. Figure 6 shows space-filling models of the oligonucleotide in which the protons that show NOE interactions with the metal complex are highlighted. It is clearly seen that, with both Δ- and Λ-$[Ru(phen)_3]^{2+}$, ligand binding exclusively involves protons lining the minor groove. From this we conclude that both enantiomers of $[Ru(phen)_3]^{2+}$ have a strong preference for binding in the minor groove of the oligonucleotide. Moreover, most of the NOE interactions observed, for both Δ- and Λ-$[Ru(phen)_3]^{2+}$, take place around the central A·T base pairs of the oligonucleotide. This demonstrates that the binding specifically occurs to the AT region of $[d(CGCGATCGCG)]_2$. However, at high $[Ru(phen)_3]^{2+}$/oligonucleotide concentration ratios (close to 1.0), and long mixing times (450 ms), weak NOEs to the H1′ protons of G2 and/or G8 were observed with Δ, indicating secondary binding sites at these positions. With the Λ enantiomer NOEs to H1′ and H4′ of the base pairs G4·C7 and C3·G8 are observed, indicating additional binding at these sites.

Experiments carried out in H_2O solution show that both the amino and imino protons in the interior of the oligonucleotide base pairs undergo rapid exchange. Rapidly exchanging imino protons are generally correlated with nonintercalative ligand binding (Feigon et al., 1984; Behravan et al., 1993). In NOESY spectra recorded at 200-ms mixing time a cross-peak between H2(A5) and the imino proton of T6 is observed (data not shown). This cross-peak may arise either from interaction within the AT base pair or from sequential interaction in the AT step, or a combination of both. Furthermore, no cross-peaks between the phenanthroline and the amino or imino protons of the oligonucleotide are seen. This is in agreement with the contention that no intercalation of the phenanthrolines takes place, since intercalation would, at least transiently, bring the phenanthroline protons close to the amino and imino protons and detectable NOEs would be expected. In attempts to detect any interaction between imino and phenanthroline protons, one-dimensional NOE experiments were carried out. The imino proton resonances were irradiated one at a time while the rest of the spectrum was observed. This resulted in no detectable intensity

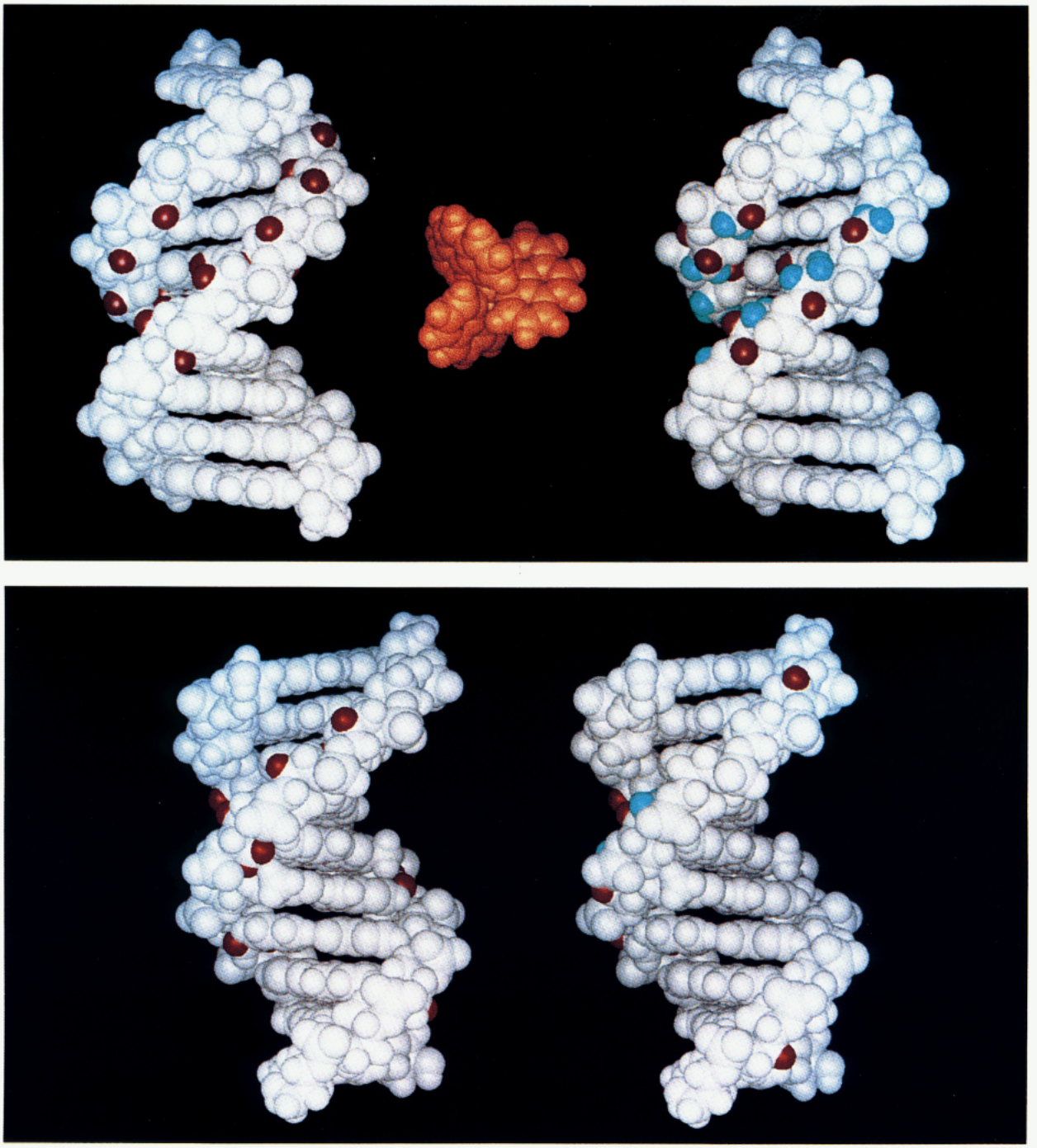

FIGURE 6: Space-filling model of $[d(CGCGATCGCG)]_2$ with protons showing NOE interactions with $[Ru(phen)_3]^{2+}$ highlighted in red and blue (ambiguous H4′/H5′/H5″ assignments). Left-hand side: interactions observed with the Λ enantiomer. Right-hand side: interactions observed with the Δ enantiomer. On the bottom are shown major groove views of the oligonucleotides and on top minor groove views, in addition to a model of Λ-$[Ru(phen)_3]^{2+}$.

changes of the phenanthroline signals. Similarly, when the phenanthroline resonances were irradiated selectively, no effects were seen in the imino proton resonances. These experiments provide further support against intercalation of the phenanthrolines.

Regarding the structure of the oligonucleotide, the NOESY data indicate that a B-conformation without any drastic disturbances is maintained during metal complex interaction. The data also indicate that no intercalative binding occurs. The intensities of the NOE cross-peaks among DNA protons were measured at several $[Ru(phen)_3]^{2+}/[d(CGCGATCGCG)]_2$ concentration ratios. It was found that the cross-peaks between consecutive residues in the aromatic–H1′ region of the NOESY show no systematic intensity variations with concentration ratio. It should also be mentioned that, with both Δ and Λ, the aromatic–H2′,H2″ regions are unperturbed and show regular continuous cross-peak connectivities along the sequence. Furthermore, in the aromatic–aromatic region sequential cross-peaks between the H6/H8 protons on G4, A5, T6, and C7 can be seen even at the higher concentration ratios, as may be seen in Figure 4. These findings argue against intercalative binding in the AT·AT and GA·TC steps, since the base pairs would be separated by some 3–4 Å by an intercalator and thus result in absent or significantly weaker sequential NOEs, as observed in studies of intercalating drug molecules (Zhang & Patel, 1990, 1991).

$[Ru(phen)_2DPPZ]^{2+}$ Studies. The interaction of the $[Ru(phen)_3]^{2+}$ analogue $[Ru(phen)_2DPPZ]^{2+}$ (III) with [d(CGC-

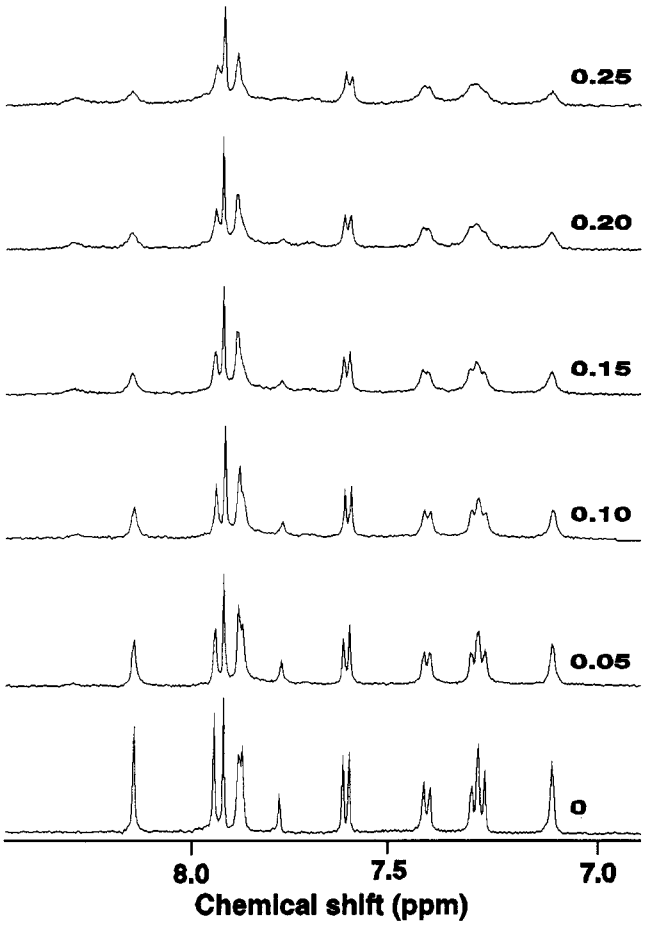

FIGURE 7: Aromatic region of the ^1H NMR spectrum of Δ-$[Ru(phen)_2DPPZ]^{2+}$ and $[d(CGCGATCGCG)]_2$ in D_2O solution at 41 °C, with r-values indicated.

$GATCGCG)]_2$ was studied with NMR. Figure 7 shows the aromatic region of the ^1H spectrum of the oligonucleotide as titrated with Δ-$[Ru(phen)_2DPPZ]^{2+}$. The resonances of H6 of T6 and of H2 and H8 of A5 all undergo considerable line broadening as the metal complex is added. This indicates that the binding kinetics are in the intermediate exchange range and are thus considerably slower for $[Ru(phen)_2DPPZ]^{2+}$ as compared to $[Ru(phen)_3]^{2+}$. This is consistent with the stronger binding of $[Ru(phen)_2DPPZ]^{2+}$ to DNA and with intercalation of the DPPZ ligand, which has previously been suggested from photophysical and linear dichroism studies (Friedman et al., 1990; Hiort et al., 1993).

CD Experiments. Circular dichroism spectra of Δ- and Λ-$[Ru(phen)_3]^{2+}$ interacting with $[d(CGCGATCGCG)]_2$, calf thymus DNA, poly(dAdT)·poly(dAdT), and poly(dGdC)·poly(dGdC) were recorded; see Figure 8. Qualitatively, the respective changes for the two enantiomers are the same when in presence of the oligonucleotide, the alternating polynucleotides, or calf thymus DNA. This strongly indicates that the metal complexes bind in the same way to the oligonucleotide as to the polynucleotides and DNA and, therefore, that the NMR and optical spectroscopy data recorded on the respective system reflect similar structures. There are, however, distinct differences between the CD changes observed for the two $[Ru(phen)_3]^{2+}$ enantiomers, implying that the spectral perturbations and, hence, the binding modes differ significantly between their respective complexes with the nucleic acids. The differences are, for example, seen in the charge-transfer region (350–550 nm). The changes in the CD signal resulting from the presence of the various nucleic acids are summarized in Table 3. With the Δ enantiomer the

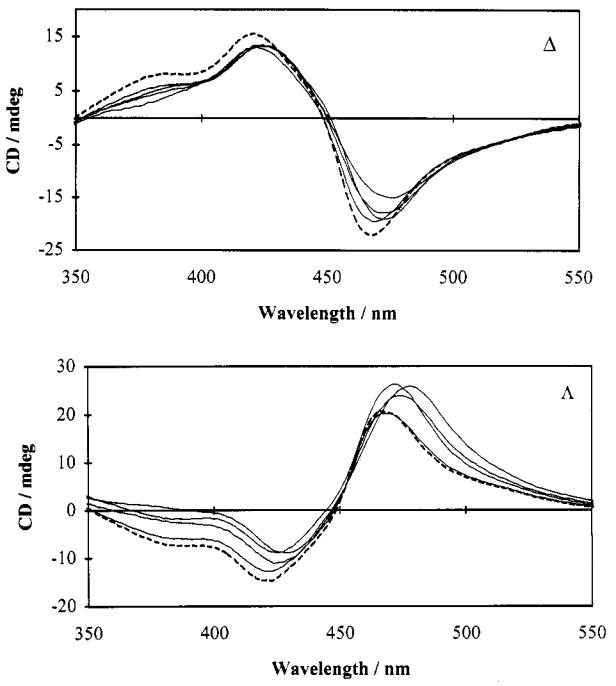

FIGURE 8: Circular dichroism spectra of $[Ru(phen)_3]^{2+}$ alone (broken curves) and in the presence of various DNAs at $[Ru(phen)_3]^{2+}$/DNA phosphate concentration ratios of 0.10, at 20 °C. The $[Ru(phen)_3]^{2+}$ concentration was 30 μM in all experiments. (Top) Solid curves denote, from bottom to top at 470 nm, Δ-$[Ru(phen)_3]^{2+}$ in the presence of $[d(CGCGATCGCG)]_2$, poly(dGdC)·poly(dGdC), calf thymus DNA, and poly(dAdT)·poly(dAdT). At 380 nm the order is reversed. (Bottom) Solid curves denote, from bottom to top, Λ-$[Ru(phen)_3]^{2+}$ in the presence of $[d(CGCGATCGCG)]_2$, poly(dGdC)·poly(dGdC), calf thymus DNA, and poly(dAdT)·poly(dAdT), at both 400 and 500 nm.

Table 3: Changes in the Charge-Transfer CD Band of $[Ru(phen)_3]^{2+}$ Interacting with Various Nucleic Acids

sample	380-nm peak[a]	420-nm peak[a]	470-nm peak[a]	point of interception[b] (nm)
Δ (pure)	100	100	100	448
Δ + AT	36	86	65	+2
Δ + GC	62	83	85	+3
Δ + ctDNA	55	83	80	+2
Δ + d(CGCGATCGCG)	71	83	89	+1
Λ (pure)	100	100	100	448
Λ + AT	−9	46	114	−2
Λ + GC	31	66	129	−5
Λ + ctDNA	23	53	114	−1
Λ + d(CGCGATCGCG)	81	86	98	−1

[a] Peak intensities given as a percentage of $\Delta\epsilon$ for $[Ru(phen)_3]^{2+}$ in the absence of nucleic acids. [b] Point of interception with $\Delta\epsilon = 0$.

amplitudes of both the positive (at 420 nm) and negative (at 470 nm) CD bands are reduced, whereas for Λ the longer wavelength band increases. From Table 3 it can also be seen that the extent of the intensity change is dependent on which type of DNA the metal complex interacts with. For both Δ and Λ the changes are most pronounced with poly(dAdT)·poly(dAdT) or poly(dGdC)·poly(dGdC). Binding to the oligonucleotide induces small changes that strongly resemble those observed in the presence of calf thymus DNA.

In the exciton region of the CD spectra, around 270 nm, only minor changes are seen when the $[Ru(phen)_3]^{2+}$ complexes are mixed with the nucleic acids (results not shown). This observation demonstrates that neither of the enantiomers undergoes any significant distortion from the octahedral geometry upon DNA binding. This is in contrast to the CD spectrum of $[Ru(phen)_2DPPZ]^{2+}$ in which considerable

changes in the exciton band are observed in the presence of nucleic acids (data not shown), indicating that structural and/or electronic changes occur upon DNA interaction.

DISCUSSION

Rapid Exchange. $[Ru(phen)_3]^{2+}$ binds to $[d(CGCGATCGCG)]_2$ with rapid exchange; i.e., the on and off rates of the ligand are high on the NMR time scale (<1 ms). The phenanthroline proton resonances are all sharp, and for the DNA protons only very limited line-broadening is seen, which is in contrast to the strong effect caused by $[Ru(phen)_2DPPZ]^{2+}$.

Apparent AT Preference. Both Δ- and Λ-$[Ru(phen)_3]^{2+}$ are found to bind preferentially to the central AT region of $[d(CGCGATCGCG)]_2$. This is evident from the NOE cross-peaks observed between the ligand and the oligonucleotide protons, which are all centered around the AT region (Figure 6). A higher affinity for AT base pairs is consistent with the more negative electrostatic potential at AT base pairs in the minor groove, as compared to GC base pairs (Pullman, 1983). The apparent AT specificity requires some comment, since there are some factors that may affect the affinity of the ligand for different parts of the oligonucleotide. From electrostatic considerations it can be expected that ligand binding is favored to the central region of an oligonucleotide. Binding to the CG base pairs of $[d(CGCGATCGCG)]_2$ might also be prevented by dynamic end effects; higher base-pair opening frequencies have been shown for the three outermost base pairs of this sequence (Leijon & Gräslund, 1992). However, $[Ru(phen)_3]^{2+}$ has been shown to bind near the ends of $[d(GTGCAC)]_2$ and at the same time raise the melting temperature of the oligonucleotide (Rehmann & Barton, 1990a). Moreover, at higher concentrations of ligand (>1.0 $[Ru(phen)_3]^{2+}$/duplex), we observe secondary interactions with base pairs near the ends of $[d(CGCGATCGCG)]_2$.

The association constants of Δ- and Λ-$[Ru(phen)_3]^{2+}$ to the AT site were found to differ significantly. It should be noticed, though, that determination of binding constants by monitoring shift changes of individual DNA protons, as done here, exclusively measures ligand association that affects the protons observed. It is thus clear that the lower binding constant obtained for the Λ enantiomer reflects a lower degree of binding to the AT region as compared to Δ but does not necessarily imply weaker binding to the whole oligonucleotide. The NOE interactions observed between the oligonucleotide and the Λ enantiomer (see Figure 6) show that binding of Λ takes place to a more extended region of the oligonucleotide and are in fact evidence for a less pronounced AT specificity, as compared to Δ.

The binding constants presented here may be compared to previously reported ones. Rehmann and Barton (1991a) found that both Δ- and Λ-$[Ru(phen)_3]^{2+}$ bind to $[d(GTGCAC)]_2$ with intrinsic binding constants (per nucleotide) of near 2.0×10^3 M^{-1} at 20 °C, which is of the same order of magnitude as the results presented here. These investigators used the chemical shift changes of the phenanthroline protons to derive the binding constants, thus not discriminating between different sites on the oligonucleotide.

The preference observed for the AT region of $[d(CGCGATCGCG)]_2$ is also consistent with binding studies of Δ- and Λ-$[Ru(phen)_3]^{2+}$ to poly(dAdT)·poly(dAdT), poly(dGdC)·poly(dGdC), and calf thymus DNA (Hiort et al., 1990). In these studies it was found that the Λ enantiomer exhibits the highest affinity for poly(dAdT)·poly(dAdT) while the Δ enantiomer prefers the mixed composition of calf thymus DNA. Possibly the Δ enantiomer has a preference for binding to a limited stretch of AT base pairs surrounded by GC base pairs, which provides a wider minor groove than poly(dAdT)·poly(dAdT). The recognized sequence might thus be $d(GATC)$ rather than $d(AT)_n$. This would also be consistent with the closer resemblance between the changes in CD spectra caused by the oligonucleotide and calf thymus DNA, as compared to the other polynucleotides. The observation that the binding of Λ to the oligonucleotide is less AT-specific than Δ suggests that the local DNA conformation is of some importance for the enantioselection of $[Ru(phen)_3]^{2+}$. It could be argued that Λ has a preference for the d(GA)·d(TC) region and therefore appears to bind over a more extended region of the oligonucleotide. This seems unlikely, however, considering the NOE contacts seen between the phenanthroline protons **2** and **3** and H2 of adenine, requiring close proximity between the nonperiferal parts of the metal complex and the edge of the AT base pairs in the minor groove. In conclusion, when binding to $[d(CGCGATCGCG)]_2$ $[Ru(phen)_3]^{2+}$ exhibits AT specificity that is more pronounced for the Δ than for the Λ enantiomer and is also dependent on the surrounding base pairs. Furthermore, the CD data indicate that a similar sequence preference may exist also for the interaction with calf thymus DNA. However, in order to gain full understanding of this matter, comparison studies with other sequences are necessary.

Minor Groove Binding. An important result from the NOE interactions observed between $[Ru(phen)_3]^{2+}$ and $[d(CGCGATCGCG)]_2$ is that, exclusively, protons located at the bottom (H2 of adenine) or on the walls (sugar protons) of the minor groove of the oligonucleotide show cross-peaks to the phenanthroline protons (cf. Figure 6). This is seen over a wide range of ligand/DNA concentration ratios, for both the Δ and Λ enantiomers. It is thus clear that binding to the minor groove of the oligonucleotide is preferred by both Δ- and Λ-$[Ru(phen)_3]^{2+}$. Even at the highest r-values studied ($r = 3.5$), no indication of any well-defined binding site in the major groove was found. Binding to the AT region in the major groove is, for electrostatic reasons, unfavorable at higher r-values, since this region of the oligonucleotide should be essentially neutralized by metal complexes associated to the minor groove and therefore less attractive.

One could argue that minor groove binding is an effect of sequence-dependent structural features of $[d(CGCGATCGCG)]_2$. However, minor groove binding appears to be preferred also with other sequences, as judged by the extensive shift changes of adenine H2 observed, for example, in the sequence $[d(GTGCAC)]_2$ (Rehmann & Barton, 1990a). Furthermore, the CD results indicate that each $[Ru(phen)_3]^{2+}$ enantiomer binds very similarly to $[d(CGCGATCGCG)]_2$ and calf thymus DNA as well as to poly(dGdC)·poly(dGdC) and poly(dAdT)·poly(dAdT), suggesting that minor groove binding is generally preferred, independent of DNA sequence.

Nonintercalative Binding. There are a number of arguments for nonintercalative binding of $[Ru(phen)_3]^{2+}$ to $[d(CGCGATCGCG)]_2$. First, in NOESY spectra sequential NOE contacts are seen in the aromatic–aromatic, aromatic–H1′, and aromatic–H2′,H2″ regions, showing that no base-pair separation takes place, as would be expected to result from intercalative binding. Second, the sequential NOE cross-peaks between the oligonucleotide protons show no intensity variations as the amount of ligand is increased. This again shows that the base-pair stacking is retained as the metal complex is bound and thus argues against phenanthroline intercalation. Third, the different binding properties seen for

$[Ru(phen)_3]^{2+}$ and $[Ru(phen)_2DPPZ]^{2+}$ are consistent with nonintercalative and intercalative binding, respectively. $[Ru(phen)_3]^{2+}$ binds relatively weakly to $[d(CGCGATCGCG)]_2$ ($K \approx 10^3$–10^4 M^{-1} in 10 mM sodium phosphate), with rapid exchange and consequently very little line broadening. $[Ru(phen)_2DPPZ]^{2+}$, in contrast, has a binding constant of 10^7–10^8 M^{-1} to calf thymus DNA under similar conditions (Hiort et al., 1993), which compares well to other known intercalators, and binds to the oligonucleotide with intermediate exchange kinetics causing extensively broadened lines in the NMR spectrum. Fourth, no NOEs are observed between the ligand protons and the amino or imino protons in the center of the base pairs or any of the aromatic or methyl protons in the major groove. A phenanthroline ligand fully or partially inserted between two base pairs would with necessity be close to some of these protons and should give rise to cross-peaks in a NOESY.

Comparison of Δ- *and* Λ-$[Ru(phen)_3]^{2+}$. There are striking similarities between the properties of the two $[Ru(phen)_3]^{2+}$ enantiomers interacting with $[d(CGCGATCGCG)]_2$. Both the Δ and Λ enantiomers are concluded to bind in the minor groove, nonintercalatively, with a preference for the AT base pairs of the oligonucleotide. However, several differences between the enantiomers are observed that should be discussed here. First, the Δ enantiomer clearly shows a stronger affinity for the AT region than does Λ. This is evident from the higher apparent binding constant to this site exhibited by Δ. Second, the chemical shift changes of DNA protons in the presence of Δ are essentially limited to the T6 residue, whereas they span over a larger part of the oligonucleotide with Λ (cf. Figure 2). Third, the DNA protons to which NOE interactions are observed are within the G4-A5-T6-C7 region with Δ but extend over C3 and G8 as well with Λ (cf. Figure 6). Fourth, there are apparently fewer interactions between the phenanthroline proton **5** of Δ and the DNA protons as compared to proton **5** of Λ. The first three points listed above show that the sequence specificities of the two enantiomers differ somewhat. While Δ strongly prefers the AT site, Λ also shows affinity for the G·C base pairs, although it still favors the AT region ahead of other sites. The fourth point, on the other hand, indicates differences in the binding modes preferred by the two enantiomers, which will be discussed below. Furthermore, linear dichroism (LD) studies have previously shown that binding of the Δ enantiomer causes a strongly reduced orientation of DNA in flow, whereas no such effect was observed with the Λ enantiomer (Hiort et al., 1990). From these LD experiments it was also concluded that the average orientation of the 3-fold symmetry axis of the $[Ru(phen)_3]^{2+}$ complex with respect to the DNA helix axis is 70° for the Δ enantiomer and 50° for the Λ enantiomer. The LD results are thus consistent with differences in the binding modes of the two enantiomers but also show that the effects on the DNA structure are somewhat different with Δ and Λ. Finally, the CD results show that nucleic acid binding has somewhat different effects on the Δ and Λ enantiomers. This is manifested by changes in their spectra that are not mirror images of one another. However, this is not a surprising observation, since binding of two enantiomers to a chiral matrix cannot be expected to result in equivalent effects.

Binding Modes. Binding of $[Ru(phen)_3]^{2+}$ to the minor groove of $[d(CGCGATCGCG)]_2$ can be imagined to occur by insertion of either one or two phenanthroline ligands into the groove. There are a number of arguments for binding of the Δ enantiomer with two phenanthroline ligands penetrating into the minor groove. First, this would explain the NOE cross-peaks observed between protons **2** and **3** on the phenanthroline and H2(A5) located at the bottom of the minor groove, whereas insertion of one phenanthroline ligand rather would result in cross-peaks involving protons **4** and **5**. Second, insertion of two ligands into the minor groove would be likely to cause minor local distortions of the oligonucleotide structure, such as unwinding and/or changes in the base-pair stacking. Such minor changes of the DNA structure may explain the observed reduction in flow orientation seen with the Δ form and could also cause the quite dramatic chemical shift changes observed for some of the aromatic DNA protons, i.e., H5 of C3 and C7. Furthermore, insertion of two phenanthroline ligands would be hydrophobically favorable since two of the hydrophobic phenanthroline ligands would essentially be displaced from the solvent. Preliminary molecular modeling experiments indicate that it is possible to fit Δ-$[Ru(phen)_3]^{2+}$ with two phenanthroline ligands inside the minor groove and that such a model in fact can account for all of the intermolecular NOEs observed at the AT site (each intermolecular cross-peak corresponds to a proton–proton distance of 5.5 Å or less).

With the Λ enantiomer there are arguments both for and against binding with two phenanthroline ligands inserted into the minor groove. The intermolecular NOE cross-peaks observed are, in analogy with the Δ enantiomer, consistent with insertion of two ligands. However, for steric reasons, as seen from preliminary molecular modeling, the Λ complex seems less likely to fit into the groove without relatively extensive distortions of the DNA structure, for which there are no indications either from NOESY or LD results.

CONCLUSIONS

The work here presented can be summarized in a number of points:

(1) Δ- and Λ-$[Ru(phen)_3]^{2+}$ both bind to the minor groove of $[d(CGCGATCGCG)]_2$ as evidenced several intermolecular NOE interactions to protons located in the minor groove and the complete lack of such interactions to protons in the major groove.

(2) The NOE data also show that both $[Ru(phen)_3]^{2+}$ enantiomers preferentially bind to the AT base pairs of $[d(CGCGATCGCG)]_2$. The AT preference is stronger for the Δ than for the Λ enantiomer, as evidenced by their different effects on the chemical shifts of the aromatic protons of adenine. This is in agreement with the NOE results, which in addition show that the Λ enantiomer exhibits some affinity for the GC base pairs flanking the AT region.

(3) Both enantiomers bind nonintercalatively, with rapid exchange, to $[d(CGCGATCGCG)]_2$, as seen from the continuous sequential NOE cross-peak pattern and the lack of NOE interactions between imino and phenanthroline protons and also in agreement with the rapid exchange kinetics which contrast with the intercalating analogue $[Ru(phen)_2DPPZ]^{2+}$ that binds with intermediate exchange rate.

(4) The modes of binding are somewhat different for the two enantiomers, as indicated by some differences in the intermolecular NOE interactions, by their apparently different effects on the DNA structure, and from the different effects the presence of DNA has on the CD spectra of Δ- and Λ-$[Ru(phen)_3]^{2+}$.

(5) Δ-$[Ru(phen)_3]^{2+}$ is proposed to bind to $[d(CGCGATCGCG)]_2$ by insertion of two of the phenanthroline ligands into the minor groove of the oligonucleotide. This would account for the intermolecular NOEs observed and be consistent with structural distortion of the DNA structure

previously observed (Hiort et al., 1991; Satayanarayana et al., 1992). Λ-$[Ru(phen)_3]^{2+}$, on the other hand, may bind with only one phenanthroline ligand in the minor groove.

(6) The binding modes of each enantiomer concluded from the oligonucleotide studies appear to be general, i.e., independent of the DNA sequence [d(CGCGATCGCG), calf thymus DNA, poly(dGdC)·poly(dGdC), or poly(dAdT)·poly(dAdT)]. This is inferred from the very similar changes in the CD spectra of the respective enantiomer in the presence of the nucleic acids.

ACKNOWLEDGMENT

We thank Mr. Per Lincoln for synthesizing the $[Ru(phen)_2DPPZ]^{2+}$ complex.

REFERENCES

Barton, J. K. (1983) *J. Biomol. Struct. Dyn. 1*, 621–632.
Barton, J. K. (1984) *Science 233*, 727–734.
Barton, J. K., & Raphael, A. (1984) *J. Am. Chem. Soc. 106*, 2466–2468.
Barton, J. K., Basile, L. A., Danishevsky, A., & Alexandrescu, A. (1984a) *Proc. Natl. Acad. Sci. U.S.A. 81*, 1961–1965.
Barton, J. K., Danishevsky, A. T., & Goldberg. J. M. (1984b) *J. Am. Chem. Soc. 106*, 2172–2176.
Barton, J. K., Goldberg, J. M., Kumar, C. V., & Turro, N. J. (1986) *J. Am. Chem. Soc. 108*, 2081–2088.
Dwyer, F. P., & Gyarfas, E. C. (1949) *J. Proc. R. Soc. N. S. W.*, 170–173.
Eriksson, M., Leijon, M., Hiort, C., Nordén, B., & Gräslund, A. (1992) *J. Am. Chem. Soc. 114*, 4933–4934.
Feigon, J., Denny, W. A., Leupin, W., & Kearns, D. R. (1984) *J. Med. Chem. 27*, 450-465.
Friedman, A. E., Chambron, J.-C., Sauvage, J.-P., Turro, N., & Barton, J. K. (1990) *J. Am. Chem. Soc. 112*, 4960–4962.
Härd, T., Hiort, C., & Nordén, B. (1987) *J. Biomol. Struct. Dyn. 5*, 89–96.
Haworth, I. S., Elcock, A. H., Freeman, J., Rodger, A., & Richards, W. G. (1991) *J. Biomol. Struct. Dyn. 9*, 23–44.
Hiort, C., Nordén, B., & Rodger, A. (1990) *J. Am. Chem. Soc. 112*, 1971–1982.
Hiort, C., Lincoln, P., & Nordén, B. (1993) *J. Am. Chem. Soc. 115*, 3438–3454.
Leijon, M., & Gräslund, A. (1992) *Nucleic Acids Res. 20*, 5339–5343.
Pullman, B. (1983) *J. Biomol. Struct. Dyn. 1*, 773–794.
Rehmann, J. P., & Barton, J. K. (1990a) *Biochemistry 29*, 1701–1709.
Rehmann, J. P., & Barton, J. K. (1990b) *Biochemistry 29*, 1709–1717.
Satayanarayana, S., Dabrowiak, J. C., & Chaires, J. B. (1992) *Biochemistry 31*, 9319–9324.
Satayanarayana, S., Dabrowiak, J. C., & Chaires, J. B. (1993) *Biochemistry 32*, 2573–2584.
Sitlani, A., Long, E. C., Pyle, A. M., & Barton, J. K. (1992) *J. Am. Chem. Soc. 114*, 2303–2312.
Zhang, X., & Patel, D. J. (1990) *Biochemistry 29*, 9451–9466.
Zhang, X., & Patel, D. J. (1991) *Biochemistry 30*, 4026–4041.